Application of reduced scale tests to improve the thermal performance of high-voltage substation connectors

C. Abomailek[1], J.-R. Riba[1*], and P. Casals-Torrens[1]

[1]Electrical Engineering Department, Universitat Politècnica de Catalunya, 08222 Terrassa, Spain

* Corresponding author: riba@ee.upc.edu; Tel.: +34-93-739-83-65

Abstract—The thermal behavior of high-voltage substation connectors is a critical aspect that must be considered during the design stage. Most research about the thermal performance of substation connector devices is based on full scale models. This paper proposes a downscaling method to evaluate the thermal performance of reduced scale substation connectors. The theoretical results attained in this paper were validated by means of FEM simulations and experimental tests. Reduced scale simulation and testing will be an essential tool for assessing the thermal performance of substation connectors and other electrical equipment during the design and validation stages.

Keywords—Scaling, thermal model, transient analysis, finite element method, short-circuit, connector.

1. INTRODUCTION

Substation connectors are among the most critical elements to take into account during the design and maintenance of an electrical substation [1]. Although being simple devices, connectors play a key role in substations, since they ensure a suitable electrical conduction between the different parts of the facility. Therefore a correct design is a matter of interest and

concern. Industry and utilities apply different international standard tests to ensure the appropriate design and performance of the new connectors [2]. These tests are aimed at ensuring a correct behavior regarding mechanical, thermal, corrosion, ageing or corona discharge performance, among others.

When designing a new device, instrument or machine, and thus before being manufactured, the new design is often fully verified by means of extensive experimental validation to ensure reliability and suitable performance, especially when mathematical models are not available. Depending on the apparatus to be designed, extensive experimental evaluation of full scale prototypes exhibit inherent drawbacks including long test times [3], low controllability, high cost [4], added complexity [5] and occasionally present a limited scope [6].

Downscale modeling and testing is a powerful tool that can partially offset these limitations, offering an attractive, simpler and economical solution. This approach can be applied in diverse engineering areas including heat transfer [3], [7], electrical [8] and mechanical [9] engineering among others. The emergence and everyday use of powerful digital software and computers has a major role and impact on design procedures and capabilities. This digital power facilitates the development of accurate and powerful design tools to generate scale models for the industry [3]. Reduced scale models, have been applied extensively in fields such as aerodynamics [10] and aeronautics [11], [12]. In the aeronautics area, subscale models are nowadays considered as an essential, valuable and viable design tools [11]. In addition, this approach possibilities systematically analyzing and adjusting the downscale models and some geometric parameters can be verified over a wide range of values [8]. Downscale prototypes must completely characterize the full-scale object in a realistic manner in order to draw equivalences between the downscale prototype and the full scale object [8]. Reduced-scale tests have also been applied in the electrical engineering area in a wide range of applications, often related to the analysis of other

phenomena, including microgrid research [13], grounding resistance calculations [14], overheat faults in gas-insulated switchgear [4], transient overvoltage distribution in power transformer windings [5], streaming currents distribution in large power transformers [15] or to perform breakdown tests in high-voltage applications [6], [8], among others.

This document proposes a new methodology to ensure a suitable thermal behavior of substation connectors based on reduced scale models and tests. To this end, the temperature rise test described in the ANSI/NEMA CC1 standard [16] and the short-time withstand current and peak withstand tests, usually known as short-circuit tests, detailed in the IEC 62271-1:2007 international standard [17] are replicated at both full and reduced scales. These reduced scale thermal tests are especially appealing for this application due to the huge power and energy requirements of the facilities and laboratories necessary to conduct such tests. Temperature rise tests and especially short-circuit tests must be performed in high-current laboratories, which have huge electrical power requirements in terms of energy consumed and instantaneous power [18]. Because of the scarcity and singularity and the laboratories required, the manufacturers habitually have to face long waiting times before tests are carried out, thus increasing manufacturing costs and time to market. Tests performed in these laboratories are also expensive [19] and not practical for the development of prototypes due to the inherent limitations of being carried out in external installations and by external technicians. These limitations can be partially overcome by means of reduced scale tests. Depending on the scaling factor, the power requirements can be much lower, materials cost minimized, sample preparation simplified and expedited and installation of the experimental setup and test times reduced due to the scaled down thermal inertia of the reduced-scale samples. To ensure appropriate thermal performance of the designed power connectors according to the requirements imposed by the international standards, it is necessary to develop suitable calculation methods to determine the values of the main parameters

such as scale, applied current or test duration among others of the reduced scale sample to be tested. By this way an equivalent thermal behavior between the downscaled and the full scale sample can be satisfied. This approach assumes that the results obtained from reduced scale tests can be extrapolated to full scale tests. Unfortunately, the scaling process is a complex task since when deriving equivalences between reduced and full scale tests, phenomena such as radiative and especially convective cooling must be analyzed carefully due to the change in the cooling rates because of the modification of the geometric dimensions [9].

Simulations based on the finite element method (FEM) are being applied for this purpose [14], [20], since this approach allows performing analyzing full and reduced scale tests with great accuracy, reduced costs and reasonable simulation times. In this paper FEM simulations are used jointly with experimental tests as a means to further validate the proposed approach since they are widely applied for virtual testing. Results provided by FEM simulations are not affected by experimental factors such as tolerances of the measuring devices or interferences due to external causes. However, there is a lack of works analyzing in detail the transient thermal behavior of downscale prototypes [3] although dynamic scaled models are appealing since they allow solving economically and accurately numerous industry problems. Previous studies have shown that scaled dynamic models can be applied for thermal problems [21].

At the knowledge of the authors of this work, dynamic reduced scale models of electrical equipment have been not reported in the electrical engineering area, this paper aiming to fill this gap. The main goal of this paper is to develop a new scaling procedure to assist the initial design of substation connectors with special emphasis on their transient thermal performance. The method developed in this work can be applied to diverse power devices such as hardware for power lines and substations, or busbars among others, to guarantee an enhanced thermal performance during operation.

2. STANDARD ELECTRO-THERMAL TESTS

The most common electro-thermal standard tests applied to substation connectors are regulated under the ANSI/NEMA CC1-2009 [16] and IEC 62271-1:2007 [17] international standards. According to the ANSI/NEMA CC1-2009, the temperature rise test evaluates the performance of the connector at 100%, 125% and 150% of the nominal current of the reference conductor of the analyzed substation connector. To pass the test, the temperature of the connector must always be lower than the temperature of the conductor, at the three current levels.

Short-circuits produce sudden electro-mechanical and thermal stresses [22]. It is, therefore, imperative to design mechanical and thermal-surge-resistant power devices to fulfill the requirements imposed by the international standards in order to minimize the risks associated to these extreme conditions. IEC 62271-1:2007 describes the most widely accepted standard procedure to test substation connectors under short-circuit occurrence. Short-circuit tests are usually performed at the estimated short-circuit current of the substation. Due to the transient nature of the short-circuit current, the mathematical expression of the short-circuit current can be described as a two-term equation, a dc-component and a steady state terms [1]. The IEC 62271-1:2007 standard proposes performing a one second short-circuit test with the highest possible transient part to reproduce the worst case short-circuit occurrence. When this is not possible because of the limitations of the power laboratory, the test can be divided in two phases. The first one or peak withstand current test, with 0.3-seconds duration, aims at reproducing the transient behavior. The second part, or short-time withstand current test, with 1-second duration and an applied current of constant amplitude tries to reproduce the thermal behavior of short-circuit.

3. TEST SCALING APPROACH AND THERMAL SIMILARITY

The following hypothesis are formulated to analyze the scaling factors,

- The final temperature of both, the full and reduced scale test samples, reached during the electro-thermal tests must be the same, since the temperature is the most influencing parameter in such tests.
- The materials of the conductor and connector remain unchanged for the samples studied in both scales.
- The torque applied to the bolting elements of the connectors is scaled to maintain the mechanical pressure applied to the apparent area of contact.

Reduced-scale tests are often based on a dynamic similarity criterion, and to define the experiemnts, dimensionless groups can be used [23][24]. Dynamic similarity is achieved when the dimensionless groups provide the same numerical results for the different scales. In the problem under analysis, this means same temperatures at same evaluation times. To achieve this goal, it is often required to change the materials of the downscale samples or the surrounding fluid, thus denaturalizing the purpose of the test. However, thermal similarity is less restrictive, since it does not imposes the characteristic dimensionless groups to have the same values [3], [25]. The tests performed at both scales are thermally similar when the homologous surfaces reach equal or homologous temperatures at homologous times [26]. To achieve this condition, the heat-flow distribution in the two scales must be similar.

A. Temperature rise test

The aim of this test is to ensure that the connector under test operates properly at the three current levels which are defined by the rated current of the reference conductor [27]. The connector passes this test when its temperature is below the temperature of the reference conductor at any current level. Downscale temperature rise tests pursue to apply the exact amount of current to reach the same steady-state temperature than that in the full scale test, for both the

connector and the reference conductor, although the rise time interval can be different for both scales.

The dimensionless groups arising from the heat conduction equation and the boundary conditions to be evaluated to ensure thermal similitude between the solid and the surrounding fluid are summarized in Table I [25].

HERE TABLE I

It is noted that the four dimensionless groups shown in Table I depend on the characteristic length of the problem, which is considered as the cubic root of the integration volume [28], and thus on the scaling factor. Dimensionless groups Π_1 and Π_2 are related to the heat conduction through the solid material and through the air due to radiative cooling. As deducted from their mathematical expressions, any scale reduction while conserving the surface temperature leads to a linear growth of the conduction term, since the distance between the solid core of the analyzed object and its surface is reduced by the scaling factor, as proved in (1).

$$\frac{\Pi_{1,RS}}{\Pi_{1,FS}} = \frac{\Pi_{2,RS}}{\Pi_{2,FS}} = \frac{k/(\sigma T_\infty^{\,3} L_{RS})}{k/(\sigma T_\infty^{\,3} L_{FS})} = \frac{L_{FS}}{L_{RS}} = n \tag{1}$$

n being the scaling factor defined as the ratio between the linear dimensions of the full scale (FS) and reduced scale (RS) test objects and T_∞ the air temperature far from the analyzed object.

The dimensionless Grashof number [29], Gr, is related to the natural convection phenomenon, since it represents the ratio between buoyancy and viscous forces in the fluid surrounding the solid object. When reducing the scale of the problem, the Gr number is also reduced as in Eq. (2).

$$\frac{Gr_{,RS}}{Gr_{FS}} = \frac{\rho_{air}^{\,2} g\beta \cdot L_{RS}^3 \cdot T_\infty / \mu^2}{\rho_{air}^{\,2} g\beta \cdot L_{FS}^3 \cdot T_\infty / \mu^2} = \frac{L_{RS}^3}{L_{FS}^3} = \frac{1}{n^3} \tag{2}$$

Finally, the Pomerantsev number, Po, is defined as the ratio between the volumetric heat sources and thermal conduction through the solid. Since the amount of volumetric heat generated

decreases with the scale of the problem, the *Po* dimensionless number also decreases as,

$$\frac{Po_{RS}}{Po_{FS}} = \frac{\dfrac{I_{RS}{}^2 R_{RS}}{k_{Al} \cdot T_C \cdot L_{C,RS}}}{\dfrac{I_{FS}{}^2 R_{FS}}{k_{Al} \cdot T_C \cdot L_{C,FS}}} = \frac{\dfrac{I_{RS}{}^2 R_{FS} \cdot n}{L_{C,FS} / n}}{\dfrac{I_{FS}{}^2 R_{FS}}{L_{C,FS}}} = \frac{1}{n} \tag{3}$$

Rearranging Eq. (3), the ratio between I_{RS} and I_{FS} can be expressed as,

$$\frac{I_{RS}}{I_{FS}} = \frac{1}{n^{3/2}} \tag{4}$$

It is noted that Eq. (4) expresses the relationship between I_{RS} and I_{FS} in order to achieve the same steady-state temperature, although the duration of the temperature rise test for both scales is different. It is noted that Eq. (4) takes into account convective and radiative effects, without any change in the materials of the scaled test objects.

B. Short-circuit test

During the short-circuit test, since the short circuit is a very fast phenomenon, the adiabatic assumption applies [19], [30]. By considering an adiabatic process, it is assumed no heat transfer, and thus the effects of conduction, radiation and convection are neglected, and thus,

$$m \cdot Cp \cdot \Delta T = I^2 R \cdot t \tag{5}$$

By assuming the same temperature rise, duration and materials for both scales, Eq. (5) results in,

$$\frac{m_{FS} \cdot Cp.\Delta T}{m_{RS} \cdot Cp.\Delta T} = \frac{\rho \cdot Cp \cdot V_{FS} \cdot \Delta T}{\rho \cdot Cp \cdot V_{RS} \cdot \Delta T} = \frac{R_{FS} \cdot I_{FS}{}^2 \cdot t}{R_{RS} \cdot I_{RS}{}^2 \cdot t} \tag{6}$$

From Eq. (6) it results,

$$\frac{V_{FS}}{V_{RS}} = \frac{R_{FS} \cdot I_{FS}{}^2}{R_{RS} \cdot I_{RS}{}^2} \tag{7}$$

Since $V_{FS} = n^3 \cdot V_{RS}$, n being the scaling factor, the relationship between the resistances for both scales becomes,

$$R_{RS} = \rho_e \cdot \frac{L_{RS}}{A_{RS}} = \rho_e \cdot \frac{L_{FS}/n}{A_{FS}/n^2} = R_{FS} \cdot n \tag{8}$$

and thus, Eq. (7) can be rewritten as,

$$\frac{n^3 \cdot V_{RS}}{V_{RS}} = \frac{R_{FS} \cdot {I_{FS}}^2}{n \cdot R_{FS} \cdot {I_{RS}}^2} \tag{9}$$

Finally, the relationship between the reduced scale and full scale currents factor for the short-circuit currents to achieve the same temperature raise with the same short-circuit duration under the adiabatic assumption can be expressed as,

$$\frac{I_{RS}}{I_{FS}} = \frac{1}{n^2} \tag{10}$$

It is noted that Eq. (4) and Eq. (10) are different because they have different purpose. Whereas Eq. (4) calculates the current ratio for the temperature rise test (considering conductive, convective and radiative phenomena) to achieve the same steady-state temperature with different duration for both scales, Eq. (10) applies the adiabatic approximation during the short-circuit transient, which pursues obtaining the same temperature by assuming the same short-circuit duration for both scales.

4. FEM MODEL

3D-FEM (Three-dimensional finite element method) is a recognized and flexible simulation tool to accurately simulate the thermal behavior of 3D devices such as sensors [31], connectors [1], bus bars [28], power transformers [33] or to model spray evaporative cooling processes [34], among others. The model applied in this research performs a Multiphysics electric-thermal analysis using the commercial Comsol® software [35]. Fig. 1 displays the mesh of the full scale substation connector analyzed in this work. The mesh of the FS connector consists of 914486 domain elements, 176608 boundary elements and 26339 edge elements, whereas the mesh of the

RS connector consists of 661724 tetrahedral elements, 133352 boundary elements and 23434 edge elements.

HERE FIGURE 1

Power losses per unit volume ($W \cdot m^{-3}$) are calculated as,

$$p_{Joule} = \vec{j} \cdot \vec{E} = \rho_e \vec{j} \cdot \vec{j} \tag{11}$$

It is noted that p_{Joule} is the heat source in the heat conduction equation [36], [37],

$$\rho Cp \frac{\partial T}{\partial t} = -\vec{\nabla} \cdot \vec{q} + p_{Joule} \tag{12}$$

By considering the electrical resistivity ρ_e to be temperature-dependent, Eq. (12) results in [38],

$$\rho Cp \frac{\partial T}{\partial t} = k\nabla^2 T + \rho_{e,293K}[1 + \alpha_e (T - 293)]\vec{j} \cdot \vec{j} \tag{13}$$

Simulations consider isotropic materials and ρ, k and Cp with constant values.

To set the initial condition of the thermal analysis, it is supposed that the test object has been acclimated to the conditions of the indoor area of test. The boundary condition at the solid/air interface including natural convection and radiation with the external ambient can be expressed as [25],

$$-\vec{n} \cdot (-k\nabla T) = h(T_\infty - T) + \varepsilon\sigma(T_\infty^4 - T^4) \tag{14}$$

$\vec{n}$ being the unit vector normal to the solid/air boundary.

Due to the complex physical phenomena involved [39], convection cooling is often analyzed from experimental data supported by dimensional analysis [40]. The convective heat transfer coefficient h is assumed to depend on temperature, thus being recalculated at each iteration of the FEM simulations. More details about the calculation of h and the 3D-FEM mode in general is found in [1].

5. ANALYZED CONNECTORS AND EXPERIMENTAL SETUP

5.1 Analyzed substation connectors

This work studies T-type mechanical substation connectors made of A356 aluminum alloy. To validate the hypothesis made in this work, full scale and reduced scale specimens are analyzed, as shown in Fig. 2. The scaling ratio n was set according to market restrictions. The first restriction is related to the commercially available HTLS (high temperature low sag) conductors, so the scaling ratio was set to n = 1.745, since this is the ratio between the diameters of the HTLS aluminum conductors dealt with. The second restriction refers to the commercially available metrics of the bolting elements, that is, M10 and M6 for the full scale and reduced scale connectors, respectively.

Whereas the full scale connector is connected to GTACSR 464 CONDOR conductors, the reduced scale connector is designed to fit with GTACSR 131-19 conductors.

HERE FIGURE 2

Tables II and III summarize the main dimensions and physical characteristics of the connectors and conductors used for both FS and RS tests.

HERE TABLE II

HERE TABLE III

5.2 Experimental Setup

The experimental setup to perform temperature rise tests consists of a bi-phase 120 kVA, 0-400 V, variable autotransformer connected to a 120 kVA step-down 400/10 V power transformer unit with output current range 0-10 kA. This equipment is placed at the AMBER laboratory of the Universitat Politècnica de Catalunya (Spain). The test loop including the analyzed substation

connectors was connected to the output of this transformer, as shown in Fig. 3. The test current was acquired by means of a calibrated Fluke i6000s-Flex Rogowski coil. Temperature was measured by means of fast Class 1 T-type thermocouples with Teflon PFA cover placed on the external surfaces of the conductors and the body of the connectors. Thermocouples were inserted in the body of the connectors by means of a small drilled hole with the help of thermal grease. Temperatures were registered every 10 seconds using an acquisition card. Temperature rise tests were conducted indoors at atmospheric conditions (12 ºC, 985.6 hPa and 56 % relative humidity). The typical tolerance of these sensors is ±0.5 ºC [41] within -40ºC ≤ T ≤ 125ºC and ±0.004·T within 125ºC ≤ T ≤ 350ºC.

HERE FIGURE 3

Experimental short-circuit tests were conducted at the facilities of Veiki VNL laboratory (Budapest, Hungary). The experimental setup to conduct such tests is able to provide up to 170 kA_{peak} and up to 1000 MVA. It consists of a protective circuit breaker, a synchronized making switch, a reactor set, two three-phase regulating transformer units and two short-circuit transformers. The output voltage and current were acquired by means of a 1kV/100V calibrated voltage divider and a calibrated Rogowski coil. Temperature was measured by means of calibrated Class 1 K-type PFA-exposed welded-tip thermocouples with a diameter of 2 mm inserted in small holes drilled in the bodies of the connectors and in the conductors. The thermocouples signals, which were registered every 100 μs, were acquired by means of a digital acquisition card through an analog converter. The typical tolerance of these sensors is ±1.5 ºC within the analyzed temperature range. Short-circuit tests were conducted outdoors at atmospheric conditions. Fig. 4 shows the loop analyzed for the short-circuit tests.

HERE FIGURE 4

6. RESULTS

This section validates the developments made in Section IV by means of FEM (finite element method simulations) and experimental results. The electro-thermal model of the FEM simulations presented in this paper are based on the models found in [1]. Experimental results are conducted by means of the setups detailed in Section V.

6.1 Temperature rise tests

This section compares the temperature evolution during the temperature rise test for both scales obtained through FEM simulations and by means of experimental results.

Due to the use of HTLS conductors, which operate at temperatures much higher than those of the traditional conductors, temperature rise tests were conducted at 100%, 110% and 120% of the rated current of the FS reference HTLS conductor, which are summarized in Table IV. Once the values of the three current steps have been settled for the FS tests, the current steps of the RS test are calculated from Eq. (4).

HERE TABLE IV

It is noted that the conductors dealt with to fit with the FS and RS connectors have been tested at 1200 A_{RMS} (GTACSR 464 CONDOR), the rated current, and at the 110% (1320 A_{RMS}) and 120% (1440 A_{RMS}) of this current. The three current steps applied to the RS tests have been scaled by applying Eq. (4), the ratio between the RS and FS current derived in this work.

Fig. 5 shows the temperature evolution of the temperature rise test for the FS and RS analyzed loops.

HERE FIGURE 5

Results in Fig. 5 show that the solutions provided by FEM simulations are in close agreement

with experimental results. It is also noted that by applying Eq. (4), the temperature rise of the RS samples is the same as in the FS samples for the three current steps thus validating the applicability and accuracy of Eq. (4).

Some FEM and experimental results are summarized and compared in Table V.

HERE TABLE V

6.2 Short-time withstand current and peak withstand test

Short-time withstand current and peak withstand tests are conducted to ensure the resilience of electrical equipment to the unpredictable and hazardous effects of short-circuit faults. Short-circuits are usually fast transient phenomena, since the electrical protections have typical actuation time less than one second. Substation connectors are tested to withstand a short-time current of several tens of kilo-amps, typically during 1 s [1]. These results provide valuable data to be used during the optimal design process of such devices. The standard short-circuit test often contains two parts, the rated peak withstand current test and the rated short-time withstand current test [17]. The connector passes the test when its temperature is less than that of the reference conductor.

Table VI summarizes the currents applied during the peak withstand current and short-time withstand current tests.

HERE TABLE VI

It is noted that from the experimental values of the FS peak withstand and short-time withstand currents, the ones related to the RS test are obtained by applying Eq. (10), which has been applied supposing adiabatic conditions.

Figs. 6 show the 0.3 s transient stage of the experimental and simulated peak withstand current test as well as the short-time withstand current test with a duration of 1 s. Figs. 6a and 6b show,

respectively, the results of FEM simulations and the experimental ones of the temperature rise and the cooling stages during the peak withstand current tests for both scales.

HERE FIGURE 6

Results presented in Fig. 6 clearly show that the connectors and conductors of both scales reach the same temperature just after the peak withstand current test, although, as expected, the RS tested components cool down faster during the cooling stage.

Figs. 7a and 7b show, respectively, FEM and experimental results of the temperature rise and the subsequent cooling phase during the short-time withstand current tests for both, the FS and RS samples analyzed.

HERE FIGURE 7

Results presented in Fig. 7 show, once again, that just after the end of the short-circuit transient, the temperature reached for the FS components is the same that of the RS components. These results validate the approach applied in Section III. Once the short-circuit current has been cleared, the cooling process for both scales has different time-constant due to the different mass of the two scales, as well as inherent differences in the convective phenomena due to the different sizes of the metallic faces in contact with the surrounding air.

Results summarized in Figs. 6 and 7 validate the applicability and accuracy of Eq. (10).

Some FEM and experimental results are summarized and compared in Table VII.

HERE TABLE VII

7. CONCLUSION

Standard thermal tests for substation connectors and many other power components, are costly, time-consuming, require very specific power laboratories, consume huge amounts of electrical

power and have an important environmental impact. By reducing the scale of the test object many of these constraints are partially mitigated since the tests can be performed in more affordable installations, which require less power. Reduced scale tests are also faster compared to full scale tests during both the installation and test stages. This paper has developed simple equations to determine the current level to match the temperature reached for the reduced scale test with that of the full scale test. Expressions to determine the required reduced scale current are provided for both the temperature rise and short-circuit standard tests. The current values obtained by means of the proposed expressions have been validated by means of FEM simulations and experimental tests conducted in high-current laboratories. FEM simulations are widely applied for virtual testing since they are faster and cheaper than real experiments while providing accurate results. Both results proved the accuracy and feasibility of the proposed reduced scale approach, thus suggesting that reduced scale simulation and testing can be a vital tool to assess the thermal performance of substation connectors and other electrical equipment during the design stage. Although the validation has been performed by using electrical loops consisting of aluminum power connectors and HTLS conductors, it can be applied to many other electrical devices such as diverse hardware for overhead power lines, busbars, or pantograph catchers for substations among many others.

ACKNOWLEDGEMENTS

The authors would like thank and SBI Connectors for providing the equipment to perform the experimental tests. They also thank the Spanish Ministry of Economy and Competitiveness and Generalitat de Catalunya for the financial support received under projects RTC-2014-2862-3 and SGR 101 2014-2016, respectively

NOMENCLATURE

$\dot{Q}$	Rate of energy with respect to time (W)
q	Heat flux density (W/m^3)
E	Electric field strength (V/m)
j	Current density (A/m^2)
C_p	Specific heat (J/(kg·K))
k	Coefficient of thermal conductivity (W/(m·K))
m	Mass (kg)
ρ	Mass density (kg/m^3)
ρ_e	Electrical resistivity (Ω·m)
α_e	Temperature coefficient of the resistivity (1/K)
R	Electrical resistance (Ω)
I	Electrical current (A)
L	Characteristic length (m)
A	Cross sectional area normal to the electrical current (m^2)
V	Volume (m^3)
h	Convective heat transfer coefficient (W/(m^2·K))
ε	Dimensionless emissivity number
σ	Stefan-Boltzmann constant (W/(m^2·K^4))
T	Absolute temperature (K)
T_o	Absolute reference temperature (K)
T_∞	Absolute air temperature far from the analyzed objects (K)
n	Scaling factor (-)

REFERENCES

[1] F. Capelli, J.-R. Riba, and J. Pérez, "Three-Dimensional Finite-Element Analysis of the Short-Time and Peak Withstand Current Tests in Substation Connectors," *Energies*, vol. 9, no. 6, p. 418, May 2016.

[2] C. Abomailek, F. Capelli, J.-R. Riba, and P. Casals-Torrens, "Transient thermal modelling of substation connectors by means of dimensionality reduction," *Appl. Therm. Eng.*, vol. 111, pp. 562–572, 2017.

[3] C. P. Coutinho, A. J. Baptista, and J. Dias Rodrigues, "Reduced scale models based on similitude theory: A review up to 2015," *Eng. Struct.*, vol. 119, pp. 81–94, 2016.

[4] H. Li, N. Shu, X. Wu, H. Peng, and Z. Li, "Scale Modeling on the Overheat Failure of Bus Contacts in Gas-Insulated Switchgears," *IEEE Trans. Magn.*, vol. 50, no. 2, pp. 305–308, Feb. 2014.

[5] Q. Yang, Y. Chen, W. Sima, and H. Zhao, "Measurement and analysis of transient overvoltage distribution in transformer windings based on reduced-scale model," *Electr. Power Syst. Res.*, vol. 140, pp. 70–77, 2016.

[6] S. A. Sebo, D. G. Kasten, T. Zhao, L. E. Zaffanella, B. A. Clairmont, and S. Zelingher, "Development of reduced-scale line modeling for the study of hybrid corona," in *Proceedings of IEEE Conference on Electrical Insulation and Dielectric Phenomena - (CEIDP '93)*, pp. 538–543.

[7] S. Rabe and B. Schartel, "The rapid mass calorimeter: Understanding reduced-scale fire test results," *Polym. Test.*, vol. 57, pp. 165–174, 2017.

[8] J. Hernandez-Guiteras, J. R. Riba, P. Casals-Torrens, and R. Bosch, “Feasibility analysis of reduced-scale air breakdown tests in high voltage laboratories combined with the use of scaled test cages,” *IEEE Trans. Dielectr. Electr. Insul.*, vol. 20, pp. 1590–1597, 2013.

[9] A. A. Alnaqi, D. C. Barton, and P. C. Brooks, “Reduced scale thermal characterization of automotive disc brake,” *Appl. Therm. Eng.*, vol. 75, pp. 658–668, 2015.

[10] F. Meinert, K. Johannessen, F. Saito, B. Song, J. Barlow, D. Burton, T. Cho, and L. F. Gouveia de Moraes, “A Correlation Study of Wind Tunnels for Reduced-Scale Automotive Aerodynamic Development,” *SAE Int. J. Passeng. Cars - Mech. Syst.*, vol. 9, no. 2, pp. 2016-01-1598, Apr. 2016.

[11] Joseph Chambers, *Modeling Flight : The role of dynamically scale*. NASA, 2015.

[12] S. Lebental, K. C. Hall, D. B. Bliss, J. Dolbow, L. E. Howle, and J. Protz, “Optimization of the aerodynamics of small-scale flapping aircraft in Hover,” Duke University, 2008.

[13] S. D. Sudhoff, S. D. Pekarek, R. R. Swanson, V. S. Duppalli, D. C. Horvath, A. E. Kasha, R. Lin, B. D. Marquet, P. R. O’Regan, H. Suryanarayana, and Y. Yan, “A reduced scale naval DC microgrid to support electric ship research and development,” in *2015 IEEE Electric Ship Technologies Symposium (ESTS)*, 2015, pp. 464–471.

[14] T. P. Hong, Q. Do Van, and T. V. Viet, “Grounding resistance calculation using FEM and reduced scale model,” in *2009 IEEE Conference on Electrical Insulation and Dielectric Phenomena*, 2009, pp. 278–281.

[15] M. A. Brubaker, S. R. Lindgren, G. K. Frimpong, and J. M. Walden, “Streaming electrification measurements in a 1/4-scale transformer model,” *IEEE Trans. Power Deliv.*, vol. 14, no. 3, pp. 978–985, Jul. 1999.

[16] ANSI/NEMA, “ANSI/NEMA CC1. Electric Power Connection for Substation.” Rosslyn, Virginia, 2009.

[17] International Electrotechnical Commission, “IEC 62271-1:2007. High-voltage switchgear and controlgear - Part 1: Common specifications.” International Electrotechnical Commission, p. 252, 2007.

[18] R. Wilkins, T. Saengsuwan, and L. O’Shields, “Short-circuit tests on current-limiting fuses: modelling of the test circuit,” *Gener. Transm. Distrib. IEE Proc. C*, vol. 140, no. 1, pp. 30–36, Jan. 1993.

[19] A. D. Polykrati, C. G. Karagiannopoulos, and P. D. Bourkas, “Thermal effect on electric power network components under short-circuit currents,” *Electr. Power Syst. Res.*, vol. 72, no. 3, pp. 261–267, Dec. 2004.

[20] F. Yang, P. Cheng, H. Luo, Y. Yang, H. Liu, and K. Kang, “3-D thermal analysis and contact resistance evaluation of power cable joint,” *Appl. Therm. Eng.*, vol. 93, pp. 1183–1192, Jan. 2016.

[21] M. H. Sabour and R. B. Bhat, “Thermal Scale Modeling by FEM and Test,” *J. Aerosp. Eng.*, vol. 23, no. 1, pp. 24–33, Jan. 2010.

[22] J. Schlabbach and K. H. Rofalski, *Power System Engineering: Planning, Design, and Operation of Power Systems and Equipment*. Weinheim, Germany: WILEY-VCH Verlag GmbH & Co., 2008.

[23] N. Ali, T. Al-Juwaya, and M. Al-Dahhan, “An advanced evaluation of spouted beds scale-up for coating TRISO nuclear fuel particles using Radioactive Particle Tracking (RPT),” *Exp. Therm. Fluid Sci.*, vol. 80, pp. 90–104, 2017.

[24] C. Lin, S.-M. Yu, W.-Y. Wong, G.-W. Tzeng, M.-J. Kao, P.-H. Yeh, V. R. Raikar, J. Yang, and T. Ching-Piao, “Velocity characteristics in boundary layer flow caused by solitary wave traveling over horizontal bottom,” *Exp. Therm. Fluid Sci.*, vol. 76, pp. 238–

252, Sep. 2016.
[25] R. L. Shannon, “Thermal Scale Modeling of Radiation-Conduction-Convection Systems,” *J. Spacecr. Rockets*, vol. 10, no. 8, pp. 485–492, Aug. 1973.
[26] T. Szirtes, P. Rózsa, T. Szirtes, and P. Rózsa, “Chapter 17 – Dimensional modeling,” in *Applied Dimensional Analysis and Modeling*, 2007, pp. 463–525.
[27] F. Capelli, J.-R. Riba, and J. Sanllehí, “Finite element analysis to predict temperature rise tests in high-capacity substation connectors,” *IET Gener. Transm. Distrib.*, vol. 11, no. 9, pp. 2283–2291, Jun. 2017.
[28] J. L. J.Oliver, M. Cervera, S. Oller, “Isotropic damage models and smeared crack analysis of concrete,” *Proc. SCI-C Comput. Aided Anal. Des. Concr. Struct.*, vol. 945958, 1990.
[29] W. Liu, J. Wang, Y. Li, Z. Zhu, D. Qie, and L. Ding, “Natural convection heat transfer at reduced pressures,” *Exp. Heat Transf.*, pp. 1–11, Jul. 2018.
[30] C. Abomailek, J.-R. Riba, F. Capelli, and M. Moreno-Eguilaz, “Fast electro-thermal simulation of short-circuit tests,” *IET Gener. Transm. Distrib.*, vol. 11, no. 8, pp. 2124–2129, Jun. 2017.
[31] S. M. Salehi, H. Karimi, R. Moosavi, and A. A. Dastranj, “Different configurations of capacitance sensor for gas/oil two phase flow measurement: An experimental and numerical study,” *Exp. Therm. Fluid Sci.*, vol. 82, pp. 349–358, Apr. 2017.
[32] M. Hamzeh, K. Sheshyekani, and G. Kadkhodaei, “Coupled electric–magnetic–thermal–mechanical modelling of busbars under short-circuit conditions,” *IET Gener. Transm. Distrib.*, vol. 10, no. 4, pp. 955–963, Mar. 2016.
[33] P. Huang, C. Mao, and D. Wang, “Analysis of electromagnetic force for medium frequency transformer with interleaved windings,” *IET Gener. Transm. Distrib.*, vol. 11, no. 8, pp. 2023–2030, Jun. 2017.
[34] N. H. Bhatt, D. Chouhan, A. R. Pati, P. Varshney, L. Das, A. Kumar, B. Munshi, A. Behera, and S. S. Mohapatra, “Role of water temperature in case of high mass flux spray cooling of a hot AISI 304 steel plate at different initial surface temperatures,” *Exp. Heat Transf.*, vol. 30, no. 5, pp. 369–392, Sep. 2017.
[35] Comsol, “COMSOL 4.3 Multiphysics User’s Guide.” COMSOL, p. 1292, 2012.
[36] M. N. Özişik, *Heat Transfer: A Basic Approach*. McGraw-Hill, 1985.
[37] Q. Liu, L. Wang, A. Mitsuishi, M. Shibahara, and K. Fukuda, “Transient heat transfer for helium gas flowing over a horizontal cylinder in a narrow channel,” *Exp. Heat Transf.*, vol. 30, no. 4, pp. 341–354, Jul. 2017.
[38] T. Dixit and I. Ghosh, “Experimental and numerical modeling of metal foam passive radiator at low temperatures,” *Exp. Heat Transf.*, vol. 31, no. 5, pp. 425–435, Sep. 2018.
[39] S. Kakaç and Y. Yener, *Convective Heat Transfer, Second Edition*. CRC Press, 1994.
[40] E. Buckingham, “On Physically Similar Systems; Illustrations of the Use of Dimensional Equations,” *Phys. Rev.*, vol. 4, no. 4, pp. 345–376, Oct. 1914.
[41] G. Yakar, “Experimental analysis of conical baffles with rifts on heat transfer and pressure drop,” *Exp. Heat Transf.*, pp. 1–11, Jun. 2018.

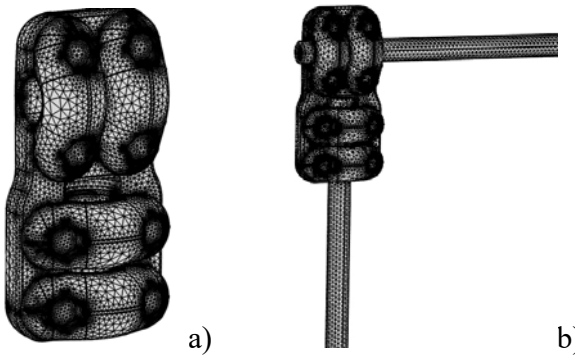

a) b)

Fig.1. a) Mesh of the S285TLS substation connector analyzed in this work. b) Mesh of the S285TLS substation connector and the related GTACSR 464 HTLS conductors.

Fig. 2. Analyzed T-type S285TLS mechanical substation connectors from SBI-Connectors catalogue. Full scale (FS) and reduced-scale (RS). The scaling factor is n = 1.745.

Fig. 3. Temperature rise tests. Test loop composed of HTLS conductors and S285ZTLS T-type mechanical substation connectors.

Fig. 4. Short-circuit tests. Test loop composed of HTLS conductors and S285TLS T-type connectors.

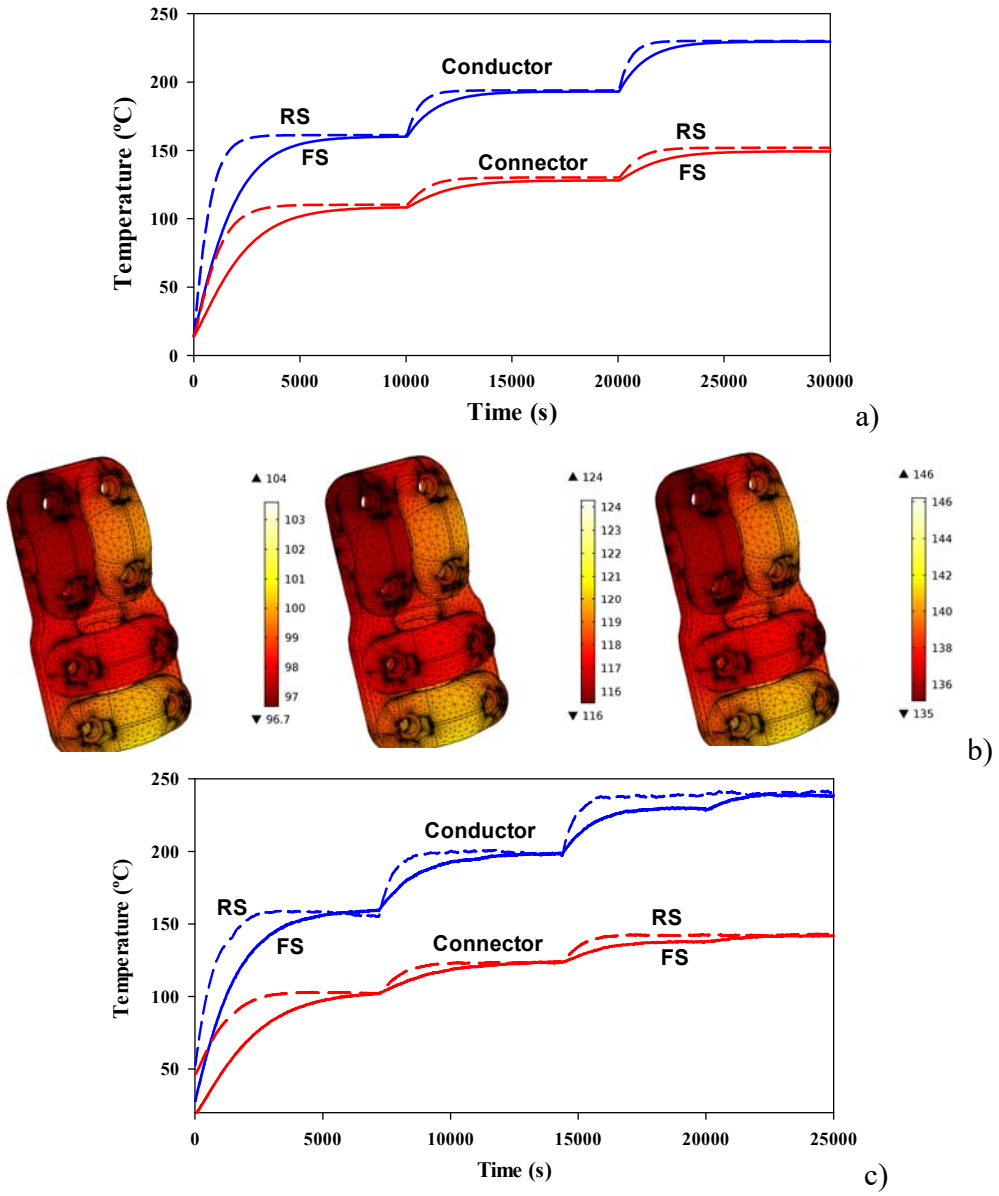

Fig. 5. Full scale and reduced scale temperature rise tests. a) FEM results. b) Thermal maps of the FS connector surface (ºC). c) Experimental results.

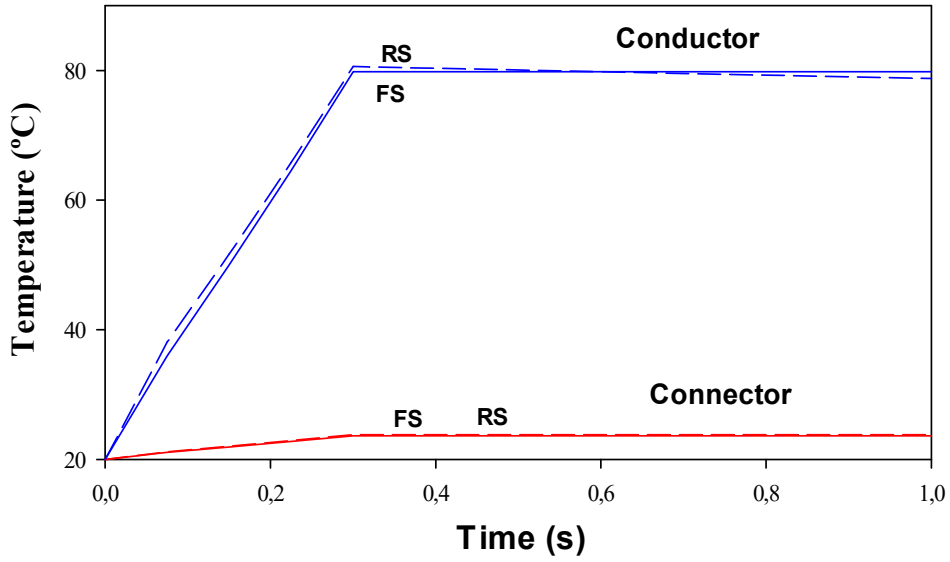
Conductor
RS
FS
Connector
FS
RS
Temperature (ºC)
Time (s)
80
60
40
20
0,0
0,2
0,4
0,6
0,8
1,0

a1)

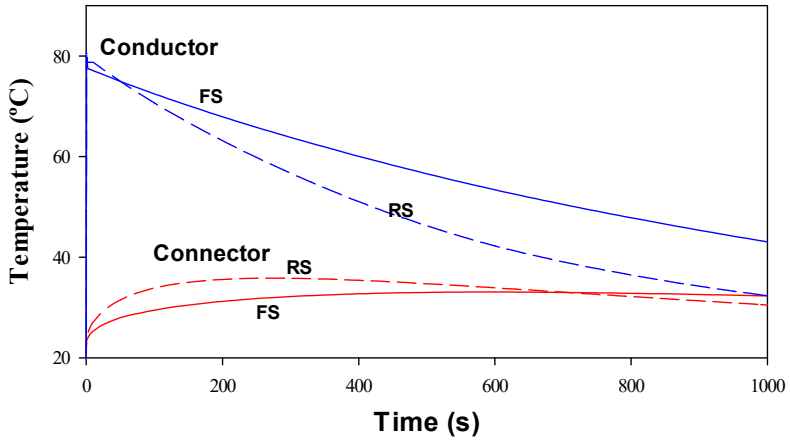
Conductor
FS
RS
Connector
RS
FS
Temperature (ºC)
Time (s)
80
60
40
20
0
200
400
600
800
1000

a2)

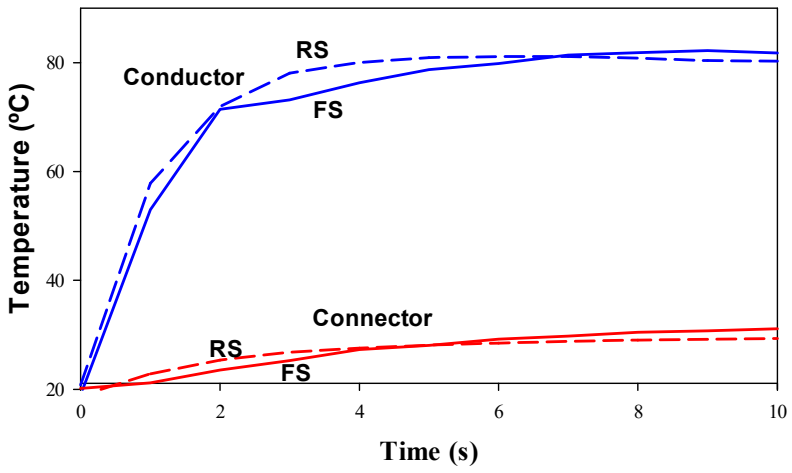
RS
Conductor
FS
Connector
RS
FS
Temperature (ºC)
Time (s)
80
60
40
20
0
2
4
6
8
10

b1)

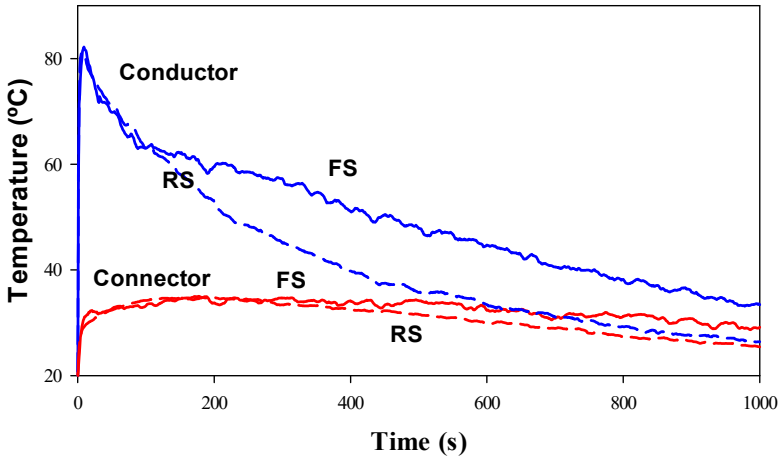

b2)

Fig. 6. Full scale and reduced scale peak withstand current test. a) FEM results. b) Experimental results.

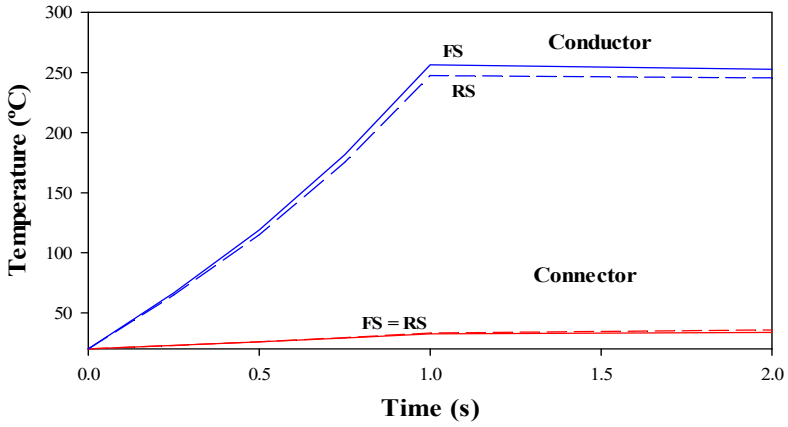

a1)

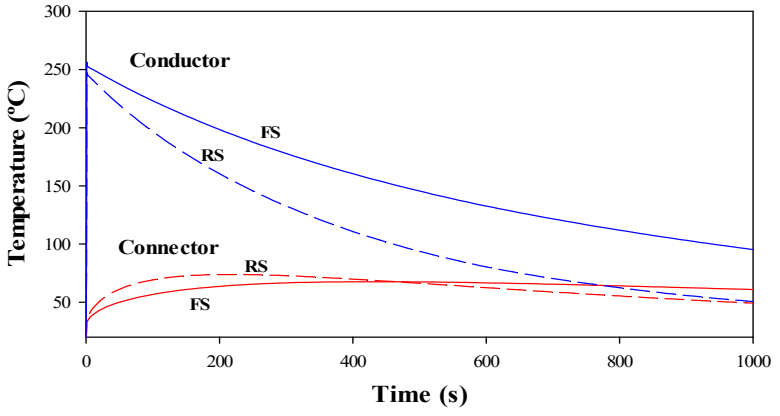

a2)

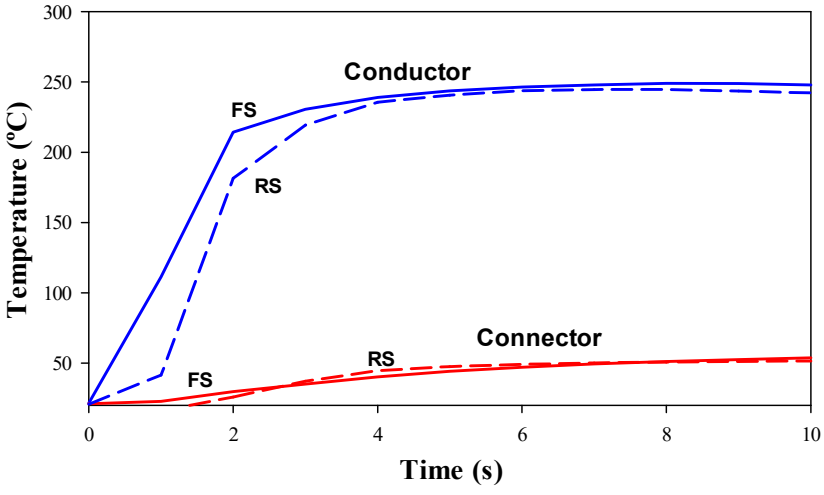

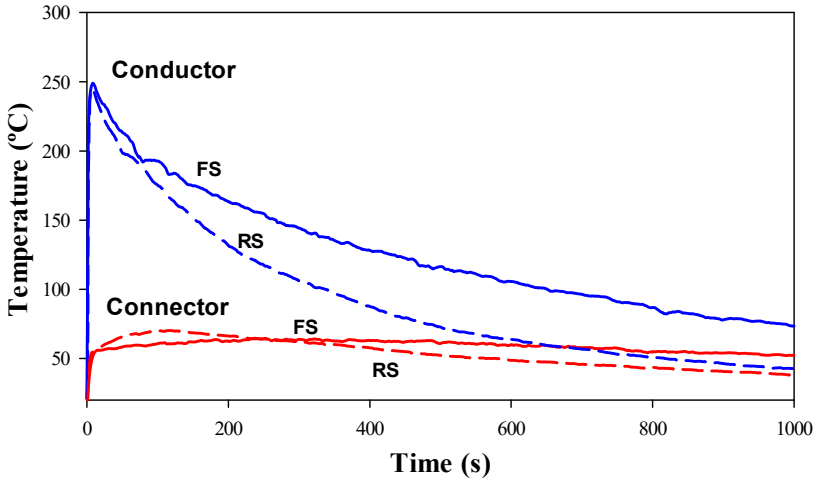

Fig. 7. Short-time withstand current test. Comparison between FS and RS tests. a) FEM results. b) Experimental results.

TABLE I
DIMENSIONLESS RELEVANT GROUPS FOR A RADIATION-CONVECTION-CONDUCTION PROBLEM

Dimensionless group	Expression	Meaning
Π_1	$\left(\frac{k_{Al}}{\sigma T_\infty{}^3 L}\right)$	Heat conduction through the solid versus radiation cooling.
Π_2	$\left(\frac{k_{Air}}{\sigma T_\infty{}^3 L}\right)$	Heat transfer to the air versus radiation cooling.
Po	$\left(\frac{L^2 p_{joule}}{k_{Al}\cdot T_\infty}\right)=\left(\frac{I^2 R}{k_{Al}\cdot T_\infty \cdot L}\right)$	Volume heat source versus conduction.
Gr	$\left(\frac{\rho_{air}{}^2 g\beta\cdot L^3\cdot T_\infty}{\mu^2}\right)$	Natural convection dimensionless number.

TABLE II
DIMENSIONS AND CHARACTERISTICS OF THE ANALYZED CONNECTORS

Variable	FS	RS
Height (mm)	188	104
Width (mm)	95	58
Maximum outer diameter (mm)	28	18
Screws and bolts metrics	M10	M6
Resistivity of aluminium alloy (Ω·m)	$4.5\cdot10^{-8}$	$4.5\cdot10^{-8}$
Temperature coefficient of resistance (ºC^{-1})	0.004	0.004
Contact resistance factor*	2	2
Dimensionless thermal emissivity factor ε (-)	0.45	0.45

*From experiments it was found that the contact resistance is twice the bulk connector resistance

TABLE III
RELEVANT DATA OF THE HTLS CONDUCTORS

Variable	FS[1]	RS[2]
Outer diameter of the conductor (mm)	27.60	15.79
Outer diameter of the steel core (mm)	9.00	5.55
Electrical resistance per unit length at 20ºC (Ω/km)	0.0708	0.2241
Temperature coefficient of resistance (ºC^{-1})	0.004	0.004
Maximum admissible temperature (ºC)	150	150
Dimensionless thermal emissivity factor ε	0.5	0.5

[1]GTACSR 464 conductor
[2]GTACSR 131-19 conductor

TABLE IV
TEMPERATURE RISE TESTS. SCALING FACTOR n = 1.745

Variable	Applied current	Step 1 100% I_n	Step 2 110% I_n	Step 3 120% I_n
Applied current (FS)	I_{FS}	1200 A	1320 A	1440 A
Applied current (RS)	$I_{RS} = I_{FS}/n^{3/2}$ (4)	520 A	573 A	625 A

TABLE V
TEMPERATURE RISE TEST. COMPARISON BETWEEN FEM AND EXPERIMENTAL CONNECTOR TEMPERATURES

Scale	Time	T_{FEM} [ºC]	$T_{Experimental}$ [ºC]
FS	Phase 1	108.4	104.2
FS	Phase 2	128.1	126.5
FS	Phase 3	149.3	142.0
RS	Phase 1	110.3	106.5
RS	Phase 2	130.1	134.4
RS	Phase 3	152.0	143.7

TABLE VI
TEST CURRENTS USED DURING THE SHORT TIME WITHSTAND CURRENT TESTS

Scale	Applied current	Peak withstand current (kA_{peak})	Short-time withstand current (kA_{RMS})
Full scale (FS)	I_{FS}	128.20	52.62
Reduced scale (RS)	$I_{RS} = I_{FS}/n^2$ (10)	42.03	17.10

TABLE VII
COMPARISON BETWEEN FEM AND EXPERIMENTAL CONNECTOR TEMPERATURES

Test and scale	$T_{MAX,FEM}$ [ºC]	$T_{MAX,Experimental}$ [ºC]
PWCT FS	33.1	35.0
PWCT RS	35.8	34.8
STWCT FS	67.6	64.8
STWCT RS	73.8	70.2

PWCT stands for peak withstand current test
STWCT stands for short-time withstand current test